Unified approach to various quantum Rabi models with arbitrary parameters*

Xiao-Fei Dong(董晓菲)[1], You-Fei Xie(谢幼飞)[1], and Qing-Hu Chen(陈庆虎)[1,2,†]

[1] *Zhejiang Province Key Laboratory of Quantum Technology and Device, Department of Physics, Zhejiang University, Hangzhou* 310027, *China*
[2] *Collaborative Innovation Center of Advanced Microstructures, Nanjing University, Nanjing* 210093, *China*

(Received 27 November 2019; accepted manuscript online 24 December 2019)

A general approach is proposed to the quantum Rabi model and its several variants within the extended coherent states. The solutions to all these models including the anisotropy and the nonlinear Stark coupling are then obtained in an unified way. The essential characteristics such as the possible first-order phase transition can be detected analytically. This approach can be easily applied to the recent experiments with various tunable parameters without much additional effort, so it should be very helpful to the analysis of the experimental data.

Keywords: exact solutions, quantum Rabi models, circuit QED, anisotropy

PACS: 03.65.Ge, 02.30.Ik, 42.50.Pq, 42.50.Lc **DOI:** 10.1088/1674-1056/ab6555

1. Introduction

The basic interaction between a two-level atom and a classical light field was described by the Rabi model many years ago.[1] Its fully quantized version in the rotating wave approximation (RWA) was introduced by Jaynes and Cummings later.[2] The Jaynes–Cummings model can be easily solved due to the conserved excitations of the atom and the photonic number. It has been widely used in the quantum optics, because the basic physics explored in the Jaynes–Cummings model alone can be realized and observed in the earlier experiments due to the extremely weak coupling between the atom and the cavity, such as Rabi oscillations, collapses and revivals of quantum state populations, quadrature squeezing, and photon anti-bunching.[3,4]

However, the situation has changed in the past decade. In many advanced solid devices, such as the circuit quantum electrodynamics (QED) system, two-dimensional electron gases, and trapped ions, the ultrastrong coupling[5,6] and even deep strong coupling[7,8] between the artificial atom and resonators have been accessed, and the RWA is demonstrated to be invalid.[5] On the other hand, the two-level system appearing in the quantum Rabi model (QRM) and its variants is a qubit, which is the building block of quantum information technologies with the ultimate goal to realize quantum algorithms and quantum computations. Just motivated by the experimental advances and potential applications in quantum information technologies, the QRM in which the RWA is not made has attracted extensive attention.[9–20] For more complete review, please refer to Refs. [21–23].

The QRM continues to inspire exciting developments in both experiments and theories recently. The anisotropic QRM[24–26] was motivated by the recent experimental progress.[27–29] It can be mapped onto the model describing a two-dimensional electron gas with Rashba (rotating wave coupling relevant) and Dresselhaus (counter rotating-wave coupling dependent) spin–orbit couplings subject to a perpendicular magnetic field.[27] These couplings can be tuned by an applied electric and magnetic field, allowing the exploration of the whole parameter space of the model. This model can directly emerge in both cavity QED[28] and circuit QED.[29] For example, in Ref. [30], a realization of the anisotropic QRM based on resonant Raman transitions in an atom interacting with a high finesse optical cavity mode was proposed. On the other hand, Grimsmo and Parkins proposed a novel scheme by adding a nonlinear coupling term to the QRM Hamiltonian.[31] This nonlinear coupling term has been discussed in the quantum optics literature under the name of dynamical Stark shift, a quantum version of the Bloch–Siegert shift, so it was later named the quantum Rabi–Stark model (RSM).[32] This model also attracted much attention in recent years.[33–35] Recently, the anisotropic Dicke model with the Stark coupling terms, which can be called as the anisotropic Dicke–Stark model, was demonstrated via cavity assisted Raman transitions in a configuration using counterpropagating laser beams.[36] For one atom case, it is just the anisotropic RSM.

With the progress on various extensions of the QRM relevant experiments, different approaches have been developed to solve various QRMs.[37] In this work, we will introduce a generical approach to solve the QRM and its several variants, such as the anisotropic QRM, RSM, and anisotropic RSM, in an unified way.

The paper is structured as follows. In Section 2, we pro-

*Project supported by the National Natural Science Foundation of China (Grant Nos. 11834005 and 11674285).
†Corresponding author. E-mail: qhchen@zju.edu.cn

pose and describe an unified analytic approach to the generalized QRM, which can be reduced to many different QRMs, using tunable coherent states. By solving the Schrödinger equation, all coefficients in the wave function can be related through the recurrence equations. The solutions for all eigenfunctions and eigenvalues of the model are obtained by locating zeros of a one-variable polynomial. The results are presented and discussed in Section 3, where the closed-form solutions for the ground-state and the first excited state are also given. The last section contains some concluding remarks.

2. Model and solutions

The general QRM can be described as follows:

$$\begin{aligned} H &= \left(\frac{1}{2}\Delta + Ua^{\dagger}a\right)\sigma_z + \omega a^{\dagger}a \\ &\quad + g_1\left(a^{\dagger}\sigma_- + a\sigma_+\right) + g_2\left(a^{\dagger}\sigma_+ + a\sigma_-\right), \end{aligned} \tag{1}$$

where Δ is the qubit energy difference, $a^{\dagger}$ (a) is the photonic creation (annihilation) operator of the single-mode cavity with frequency ω, g_1 and g_2 are the rotating wave and counter rotating-wave coupling constants, respectively, σ_k $(k = x, y, z)$ are the Pauli matrices, and U is the nonlinear Stark coupling strength. Set $r = g_2/g_1$ as the anisotropic parameter. Note that if $U = 0$, it is the original QRM for $g_1 = g_2$ and anisotropic QRM for $g_1 \neq g_2$, while if $U \neq 0$, it is no other then RSM for $g_1 = g_2$ and anisotropic RSM for $g_1 \neq g_2$. If $r = 0$, these models are reduced to their RWA counterparts. Therefore, equation (1) describes the most general and also the most complicate model.

Fortunately, associated with this very general Hamiltonian is still the conserved parity $\Pi = \exp(\mathrm{i}\pi\widehat{N})$, $[\Pi, H] = 0$, where $\widehat{N} = (1+\sigma_z)/2 + a^{\dagger}a$ is the total excitation number. Π has two eigenvalues ± 1, depending on whether $\widehat{N}$ is even or odd. Due to this parity symmetry, we can study the general model (1) with the same scheme.

First, we employ the following transformation:

$$P = \frac{1}{\sqrt{2}}\begin{pmatrix} \sqrt{r} & 1 \\ -\sqrt{r} & 1 \end{pmatrix}, \quad P^{-1} = \frac{1}{\sqrt{2}}\begin{pmatrix} \frac{1}{\sqrt{r}} & -\frac{1}{\sqrt{r}} \\ 1 & 1 \end{pmatrix}, \tag{2}$$

then Hamiltonian (1) can be written as a matrix below (in units of $\omega = 1$):

$$H_1 = PHP^{-1} = \begin{pmatrix} a^{\dagger}a + \beta a + \frac{\lambda_+}{\beta}a^{\dagger} & -\left(\frac{1}{2}\Delta + Ua^{\dagger}a\right) - \frac{\lambda_-}{\beta}a^{\dagger} \\ -\left(\frac{1}{2}\Delta + Ua^{\dagger}a\right) + \frac{\lambda_-}{\beta}a^{\dagger} & a^{\dagger}a - \beta a - \frac{\lambda_+}{\beta}a^{\dagger} \end{pmatrix}, \tag{3}$$

where $\lambda_{\pm} = \left(g_1^2 \pm g_2^2\right)/2$ and $\beta = \sqrt{g_1 g_2}$.

Next, we expand the eigenfunction as

$$|\Psi\rangle = \begin{pmatrix} \sum_{n=0}^{\infty} c_n \left(a^{\dagger}\right)^n \exp\left(\alpha a^{\dagger}\right)|0\rangle \\ \Pi \sum_{n=0}^{\infty} c_n \left(-a^{\dagger}\right)^n \exp\left(-\alpha a^{\dagger}\right)|0\rangle \end{pmatrix}, \tag{4}$$

where α is the tunable displacement of the coherent states and each term can be regarded as an extended coherent state.

By the Schrödinger equation, we have the same following equation for both up and down levels due to the conserved parity:

$$\begin{aligned} &\left[a^{\dagger}a + \beta a + \frac{\lambda_+}{\beta}a^{\dagger}\right]\sum_{n=0}^{\infty} c_n \left(a^{\dagger}\right)^n \exp\left(\alpha a^{\dagger}\right)|0\rangle \\ &-\Pi\left[\left(\frac{1}{2}\Delta + Ua^{\dagger}a\right) + \frac{\lambda_-}{\beta}a^{\dagger}\right] \\ &\times \sum_{n=0}^{\infty} c_n \left(-a^{\dagger}\right)^n \exp\left(-\alpha a^{\dagger}\right)|0\rangle \\ &= E\sum_{n=0}^{\infty} c_n \left(a^{\dagger}\right)^n \exp\left(\alpha a^{\dagger}\right)|0\rangle. \end{aligned}$$

Each term in both sides of the above equation can be grouped into terms in $(a^{\dagger})^m \exp\left(\alpha a^{\dagger}\right)|0\rangle$. Equating the coefficients of these terms in m-th order yields

$$\begin{aligned} Ec_m &= (m + \beta\alpha)c_m + \left(\alpha + \frac{\lambda_+}{\beta}\right)c_{m-1} + (m+1)\beta c_{m+1} \\ &\quad - \Pi(-1)^m \sum_{j=0}^{m} \frac{(2\alpha)^j}{j!}\left\{\left[\frac{\Delta}{2} + U(m-j)\right]c_{m-j} \right. \\ &\quad \left. + \left(U\alpha - \frac{\lambda_-}{\beta}\right)c_{m-j-1}\right\}. \end{aligned} \tag{5}$$

Similar to Refs. [34,38], looking at the eigenfunction (4), one can note that c_0 is flexible in the Schrödinger equation where the normalization for the eigenfunction is not necessary, so we select $c_0 = 1$. The linear term in $a^{\dagger}$ in the Fock space can be also determined by the displacement α in the pure coherent state, so we do not need c_1, which can be set to zero. The constant term in Eq. (5) by $m = 0$ gives the relation between the energy and the tunable parameter α,

$$E = \beta\alpha - \frac{\Pi}{2}\Delta. \tag{6}$$

Inserting Eq. (6) into Eq. (5) leads to the following recursive relation for coefficients c's:

$$\begin{aligned} c_{m+1} &= \frac{\left(m + \frac{\Delta}{2}\Pi\right)c_m + \left(\alpha + \frac{\lambda_+}{\beta}\right)c_{m-1}}{-(m+1)\beta} \\ &\quad + \frac{\Pi(-1)^m}{(m+1)\beta}\sum_{j=0}^{m}\frac{(2\alpha)^j}{j!}\left\{\left[\frac{\Delta}{2} + U(m-j)\right]c_{m-j} \right. \\ &\quad \left. + \left(U\alpha - \frac{\lambda_-}{\beta}\right)c_{m-j-1}\right\}. \end{aligned} \tag{7}$$

For any real physical systems, the wavefunction should be analytic and well defined, so the higher order coefficients should be vanishingly small. Strictly speaking, $c_{m\to\infty}\to 0$. But in the real calculation, one cannot set m to infinite as the numerical diagonalization proceeds in the truncated Hilbert space. Thus we need truncate the summation by setting $c_{m_{\rm tr}+1}=0$. $c_{m_{\rm tr}+1}$ is actually a polynomial in α, also in the energy E if using relation (6). The zero locations of Eq. (7) converge reasonably well with increasing truncated number $m_{\rm tr}$. In principle, we can set infinite truncated number, but it is impossible to implement practically in the numerical calculations. All the coefficients can be obtained by this E-dependent polynomial equation, thus the eigenstates (4) can be also obtained. We actually can determine the solutions of the model with any desired accuracy by increasing truncated number $m_{\rm tr}$. The solutions are demonstrated in the next section for arbitrary model parameters in various quantum Rabi models.

3. Results and discussion

Most importantly, for arbitrary model parameters, the saturation calculation can be arrived at if $m_{\rm tr}$ is large enough, which results in exact solutions. It is very crucial to obtain the real roots of Eq. (7) for sufficient large truncation number $m_{\rm tr}$. We plot a two-dimensional diagram $c_{m_{\rm tr}+1}(E)$. The schematic view of the solutions for the one-variable polynomial equation $c_{m_{\rm tr}+1}(E)$ with different model parameters in the most general model (1) are presented in Fig. 1. The real roots are just the intersection points of the curve and abscissa axis. The crossing points are just the solutions for eigenvalues E. Here the relative difference of the energy is less than 10^{-6} for all coupling strengths if $m_{\rm tr}$ is around 40. To confirm that all obtained eigenvalues are true ones of the model, we perform the numerical exact diagoanlizations (ED) in the Fock space. The ED results are indicated by the open circles. Excellent agreement is found for various parameters.

By this method, we can further calculate the energy spectra for the general model (1) with arbitrary parameters. In Fig. 2, we plot the spectra for $\Delta=0.5$, $U=0.5$, and $r=0.5$. The numerical ED results are also exhibited with open circles. Both results are almost the same. Interestingly, the first two energy levels cross at one point. The level crossing just indicates the first-order quantum phase transition, because the first derivative of the lowest energy is discontinuous at this crossing point.

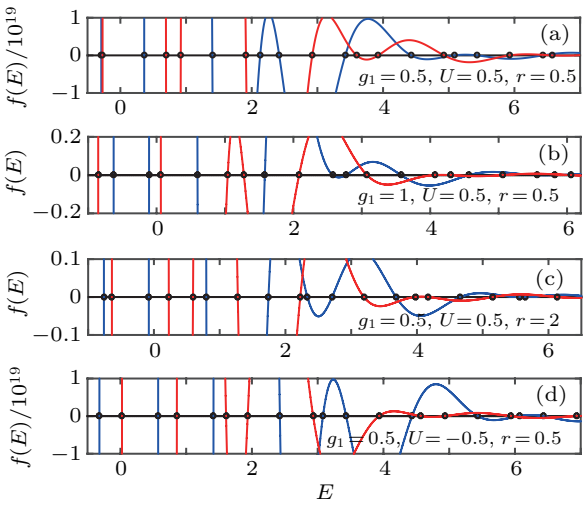

Fig. 1. Schematic view of the solutions for the one-variable (E) polynomial Eq. (7) with (a) $g=0.5$, $U=0.5$, $r=0.5$; (b) $g=1$, $U=0.5$, $r=0.5$; (c) $g=0.5$, $U=0.5$, $r=2$; and (d) $g=0.5$, $U=-0.5$, $r=0.5$. Even parity is denoted by blue and odd parity by red. The black circles are numerical ED solutions for the energy. $\Delta=0.5$.

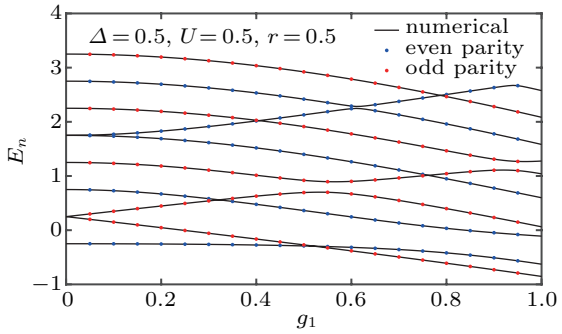

Fig. 2. Energy spectra for $\Delta=0.5$, $U=0.5$, $r=0.5$ by both present approach (solid lines) and the numerical ED (black circles).

In the studies of the original simplest QRM, the analytical closed-form solution is very interesting and helpful.[39,40] Now, in our unified framework, we can also present the closed-form solutions to this general model by terminating the summation in Eq. (7) at $m_{\rm tr}=2$, i.e., $c_3=0$, which yields

$$\alpha^2+\frac{\left(1-U^2-U\Delta+\Pi\Delta-2\Pi\lambda_-\right)}{\beta\Pi\left(2U+\Delta\right)}\alpha +\frac{\left(\lambda_+-\lambda_-\Pi\right)\left(1-\Pi U\right)}{\beta^2\Pi\left(2U+\Delta\right)}=0,$$

then we have

$$\alpha^{\pm}=-\frac{\left(1-U^2-U\Delta+\Pi\Delta-2\Pi\lambda_-\right)}{2\beta\Pi\left(2U+\Delta\right)}\pm\sqrt{\frac{\left(1-U^2-U\Delta+\Pi\Delta-2\Pi\lambda_-\right)^2}{4\beta^2\left(2U+\Delta\right)^2}-\frac{\left(\lambda_+-\lambda_-\Pi\right)\left(1-\Pi U\right)}{\beta^2\Pi\left(2U+\Delta\right)}}.$$

Checking with numerics, we obtain the first energy for even and odd parity in the closed-form, respectively

$$E_{\Pi=1}=\frac{U^2-U\Delta-\Delta-1+2\lambda_--\Delta^2}{2\left(2U+\Delta\right)}+\sqrt{\frac{\left(1-U^2-U\Delta+\Delta-2\lambda_-\right)^2}{4\left(2U+\Delta\right)^2}-\frac{\left(\lambda_+-\lambda_-\right)\left(1-U\right)}{2U+\Delta}},\tag{8}$$

$$E_{\Pi=-1} = \frac{U^2 - U\Delta + \Delta - 2\lambda_- - \Delta^2 - 1}{-2(2U+\Delta)} - \sqrt{\frac{(1-U^2-U\Delta-\Delta+2\lambda_-)^2}{4(2U+\Delta)^2} + \frac{(\lambda_+ + \lambda_-)(1+U)}{(2U+\Delta)}}. \tag{9}$$

Also considering the most complicate case, i.e., nonzero U and $r \neq 1$, we plot the above two energies Eqs. (8) and (9) in Fig. 3 for $\Delta = 0.5, U = 0.5, r = 0.1$. The first 4 energy levels from the exact solutions are also displayed for comparison. The level crossing of the first two exact energy levels also appears in the corresponding closed-form solutions. Although deviating from the true crossing point, the qualitative feature is still captured in the simple closed-form study. One may note that the present closed-form solution is only a second-order approximation, but the essential feature of the model is still included. It may highlight that in the present ansatz (4), only a few terms in the expansion can dominate the true one.

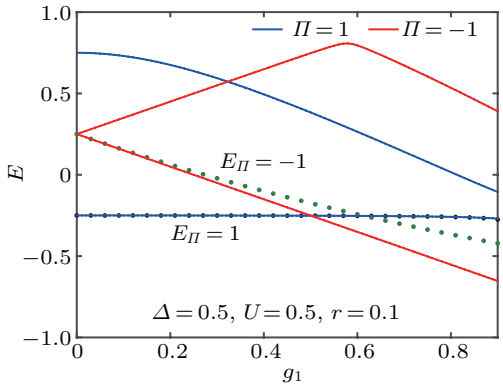

Fig. 3. A few low levels for $\Delta = 0.5$, $U = 0.5$, $r = 0.1$ by both the closed form (filled circles) and the exact solutions by zeros of Eq. (7) (solid lines). Level crossing appears for both cases.

In the recent experiments, many solid-state devices can be operated in the ultra-strong cavity–cavity coupling regime, i.e., $g < 0.2$. From Fig. 3, one may see that the closed-form solutions are very close to the true ones up to the ultra-strong coupling regime. This situation becomes even better for the ground-state energy. In Fig. 4, we plot the ground state energy up to $g = 0.5$ by Eq. (8). An excellent agreement in wider coupling regime is obviously exhibited.

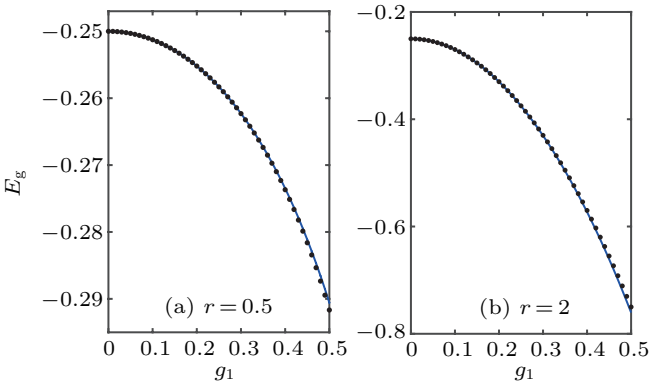

Fig. 4. Comparisons of the ground-state energies by the present closed form solution (filled circles) and the exact solutions by zeros of Eq. (7) (solid curves) for $\Delta = 0.5$, $U = 0.5$, (a) $r = 0.5$ and (b) $r = 2$ (right).

4. Conclusion

We have proposed a unified approach to the quantum Rabi model and its several variants. A polynomial equation with a single variable is derived by tunable extended coherent states for the most general model, which is more complicate than the often studied models. The solutions to this polynomial equation recover exactly all eigenvalues and eigenfunctions of the models for arbitrary model parameters. Closed-form solutions are also given for the first two levels, which are very accurate up to the ultrastrong coupling regime. The first-order quantum phase transitions for some parameters are observed in the unified exact solutions, and also appear in the closed-form ones. Further physics phenomena in the presence of anisotropy and nonlinear Stark coupling will be explored within this unified scheme in the near future.

Finally, we like to point out that this unified method should be very helpful to analyze the experimental data in the recent circuit QED systems from the weak coupling, ultrastrong coupling, and deep-strong coupling regimes. For some experimental device, the underlying interactions information such as anisotropy and nonlinearity are not very clear, and thus the specified model is unknown *in priori*. By using the present universal approach, one can easily fit the experiential data to the theoretical results based on the generalized model where all possible interactions are taken into account, and finally detect the real interactions in the experiments.

References

[1] Rabi I I 1937 *Phys. Rev.* **51** 652
[2] Jaynes E T and Cummings F W 1963 *IEEE Proc.* **51** 89
[3] Scully M O and Zubairy M S 1997 *Quantum Optics* (Cambridge: Cambridge University Press)
[4] Orszag M 2007 *Quantum Optics Including Noise Reduction, Trapped Ions, Quantum Trajectories, and Decoherence* (Science Publish)
[5] Niemczyk T, Deppe F, Huebl H, Menzel E P, Hocke F, Schwarz M J, Garcia-Ripoll J J, Zueco D, Humer T, Solano E, Marx A and Gross R 2010 *Nat. Phys.* **6** 772
[6] Forn-D Píaz, Lisenfeld J, Marcos D, Garca-Ripoll J J, Solano E, Harmans C J P M and Mooij J E 2010 *Phys. Rev. Lett.* **105** 237001
[7] Yoshihara F, Fuse T, Ashhab S, Kakuyanagi K, Saito S, and Semba K 2016 *Nat. Phys.* **13** 44
[8] Forn-D Píaz, García-Ripoll J J, Peropadre B, Orgiazzi J L, Yurtalan M A, Belyansky R, Wilson C M and Lupascu A 2016 *Nat. Phys.* **13** 39
[9] Casanova J, Romero G, Lizuain I, García-Ripoll J J and Solano E 2010 *Phys. Rev. Lett.* **105** 263603
[10] Braak D 2011 *Phys. Rev. Lett.* **107** 100401
[11] Chen Q H, Wang C, He S, Liu T and Wang K L 2012 *Phys. Rev. A* **86** 023822
[12] He S, Wang C, Chen Q H, Ren X Z, Liu T and Wang K L 2012 *Phys. Rev. A* **86** 033837
[13] He S, Zhao Y and Chen Q H 2014 *Phys. Rev. A* **90** 053848
[14] Zhong H H, Xie Q T, Batchelor M and Lee C H 2013 *J. Phys. A* **46** 415302
[15] Maciejewski A J, Przybylska M and Stachowiak T 2014 *Phys. Lett. A* **378** 3445

[16] Chen Q H, Zhang Y Y, Liu T and Wang K L 2008 *Phys. Rev. A* **78** 051801

[17] Gan C J and Zheng H 2010 *Eur. Phys. J. D* **59** 473

[18] Ying Z J, Liu M X, Luo H G, Lin H Q and You J Q 2015 *Phys. Rev. A* **92** 053823

[19] Hwang M J, Puebla R and Plenio M B 2015 *Phys. Rev. Lett.* **115** 180404

[20] Liu M X, Chesi S, Ying Z J, Chen X S, Luo H G and Lin H Q 2017 *Phys. Rev. Lett.* **119** 220601

[21] Braak D, Chen Q H, Batchelor M and Solano E 2016 *J. Phys. A: Math. Gen.* **49** 300301

[22] Gu X, Kockum A F, Miranowicz A, Liu Y X and Nori F 2017 *Phys. Rep.* **718–719** 1

[23] Forn-Díaz P, Lamata L, Rico E, Kono J and Solano E 2019 *Rev. Mod. Phys.* **91** 25005

[24] Yu Y X, Ye J and Liu W M 2013 *Sci. Rep.* **3** 3476

[25] Xie Q T, Cui S, Cao J P, Amico L and Fan H 2014 *Phys. Rev. X* **4** 021046

[26] Tomka M, Araby O. E, Pletyukhov M and Gritsev V 2014 *Phys. Rev. A* **90** 063839

[27] Erlingsson S I, Egues J C and Loss D 2010 *Phys. Rev. B* **82** 155456

[28] Schiroa M, Bordyuh M, Otu ztop B and Tureci H E 2012 *Phys. Rev. Lett.* **109** 053601

[29] Wallraff A, Schuster D I, Blais A, Frunzio L, Huang R S, Majer J, Kumar S, Girvin S M and Schoelkopf R J 2004 *Nature* **431** 162

[30] Grimsmo A L and Parkins S 2013 *Phys. Rev. A* **87** 033814

[31] Grimsmo A L and Parkins S 2014 *Phys. Rev. A* **89** 033802

[32] Eckle H P and Johannesson H 2017 *J. Phys. A: Math. Theor.* **50** 294004

[33] Xie Y F, Duan L W and Chen Q H 2019 *J. Phys. A: Math. Theor.* **52** 245304

[34] Xie Y F and Chen Q H 2019 *Commun. Theor. Phys.* **71** 623

[35] Cong L, Felicetti S, Casanova J, Lamata L, Solano E and Arrazola I 2019 arXiv:1908.07358

[36] Zhang Z Q, Lee C H, Kumar R, Arnold K J, Masson S J, Grimsmo A L, Parkins A S and Barrett M D 2018 *Phys. Rev. A* **97** 043858

[37] Xie Q T, Zhong H H, Batchelor M T and Lee C H 2016 *J. Phys. A: Math. Theor.* **50** 113001

[38] Chen Q H, Liu T, Zhang Y Y and Wang K L 2011 *Europhys. Lett.* **96** 14003

[39] Feranchuk I D, Komarov L I and Ulyanenkov A P 1996 *J. Phys. A* **29** 4035

[40] Irish E K 2007 *Phys. Rev. Lett.* **99** 173601